

A tool for Pathologists to Identify diseased lungs from Chest X-rays using DLBLIIT

¹Dr. M. MUTHURAMAN

¹Assistant Professor, P.G. and Research Department of Computer Science, H.H. The Rajah's College (A), Pudukkottai, muthuraman70@gmail.com

Abstract

Cases of LDs (Lung Diseases) are increasing rapidly. In most disease that affects humans LDs have proven to be fatal in many cases including the current wave of Corona. More than one lakh Indians are affected perennially as LDs have a propensity to remain asymptomatic, especially in the early stages, making detection practically impossible. As a result, early detection of LDs can play a crucial role in saving lives since they provide patients higher chances of treatments where technologies can play critical roles. Based on these findings, several researchers have offered various ways of using CADs (Computer Aided Diagnostics) where MLTs (Machine Learning Techniques) including DLTs (Deep Learning Techniques) have been used. Furthermore, numerous approaches based on IPTs (Image Processing Techniques) have also predicted malignancy levels of lungs. Hence, this paper aims to detect LDs using DLTs. Experimental results of the proposed approach were found to be above ninety percent in terms of accuracy of detections.

Keywords: Lung disease classification, Convolution Networks, Deep learning, Machine Learning.

INTRODUCTION

In global figures of perennial deaths, LDs top the list with very high mortality rates. LDs are mostly respiratory diseases that affect lung's airways and other structures [1]. Roughly 1 million of adults require hospitalization because of LDs and around 50,000 die from LDs annually only in US which include tuberculosis, asthma, pneumonia, lung cancers which affect millions of people around the world (Forum of International Respiratory Societies) [2]. COVID the current pandemic is also a LD that has global impacts [3], straining healthcare systems around the world [4]. Figure 1 depicts global counts of chronic people affected with respiratory ailments.

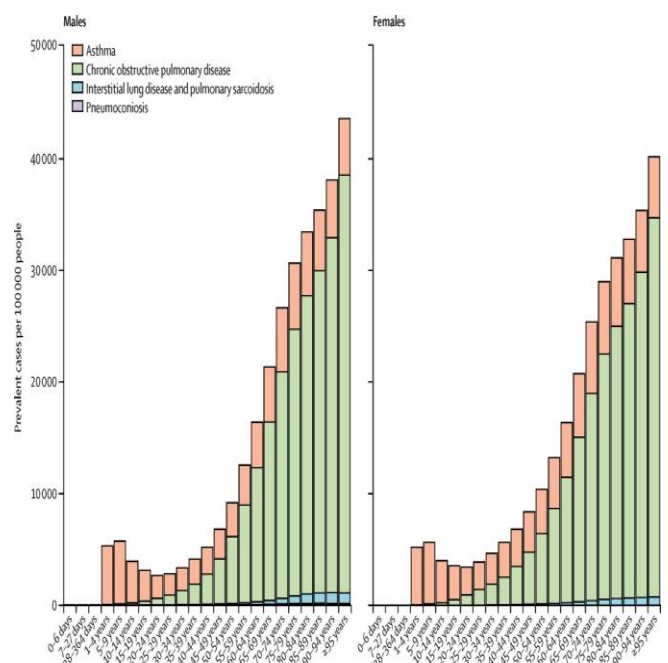


Fig. 1 - Global age/sex specific prevalence of chronic respiratory diseases

Traditionally, LDs were detected by examining blood/sputum samples [5] or imagery like CXRs (Chest X-Rays) and CTSs (Computed Tomography Scans) [6]. CXRs are one of the most frequently used diagnostic modality in detecting different LDs. CXRs can play a primary role in diagnostics of LDs and thus help in early therapies for LDs [7]. Technological improvements have also been evolving in parallel to healthcare improvements where the use of DLTs which mimic the human brain has led to enhanced medical applications. These have been tested on identifications, quantifications and classifications of patterns from complex medical imagery [8] where they identify features from raw/unprocessed data. In healthcare, DLTs are seen as substitutions for hand designed feature identifications or domain-specific knowledge and can be of significant help in categorizing medical ailments [9]. Examination of lung deformities when seen in CXRs may be missed as not all of them are visible in retrospect. Studies show that at least 15% of LDs cases are missed. To address this problem researchers have been proposing many techniques [10]. Hence, this research work proposes DLT model to address the problem of early LD detection. The approach based on deep learning called DLBLDIT (Deep Learning Based Lung Diseases Investigation Technique) identifies LDs from CXRs for early treatment and cure. The basic idea behind training DLTs using CXRs as inputs is to evaluate its identification of LDs matched with expert's identification of LDs. Following this introductory section, the next section is a review of studies related to LD identifications from medical images and DLTs that have been used. The third section presents the methodology while the fourth sections display results of the proposed scheme. This paper concludes with section five.

Research Related Studies:

In Histopathologies, specimen of biopsies, mounted on glass slides are studies for identifying diseases where human body tissues are stained with dyes for clarity of its elements.

Images of lungs for Histopathology can be captured by multitude of imaging modalities including CTSs, PETs (Positron Emission Tomographies), MRIs (Magnetic Resonance images) and CXRs. These modalities produce diagnostic pictures that aid physicians in identifying medical abnormalities and thus help in appropriate treatments [11]. CXR pictures are the most often used for reproducing conditions of blood vessels, airway passages, hearts, spinal chords/bones and other internal parts. CXRs are traditional photographic films, which need processing for examinations and hence can be automated [12] for identification of abnormalities like Tuberculosis [13], pneumonia [14], lung cancers [15], and COVID [16]. Figure 2 displays the CXRs of normal Lungs.

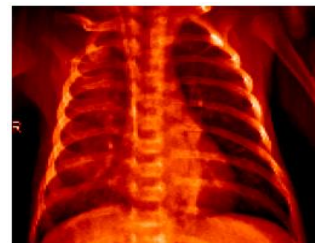


Fig. 2 - Normal Lung CXR

CTSs are radiographic images that are used by computer processes to create sectional images with varying depths and captured around the patient's body from various angles. These picture slices can be viewed singularly or layered together to create 3D depictions of tissues/organs/skeletons and thus identify body part's abnormalities [17]. Though CTSs can deliver more information, CXRs are more widely used. Figure 3 depicts a CTS Image.



Fig. 3 - CTS Image

AI (Artificial intelligence) and DLTs can transform disease diagnostics and their therapies using complex classifications that are

difficult for human experts who need to rapidly review immense amounts of images. Traditional algorithmic approaches i classify based on manual identification for segmenting identified objects were statistical measures or shallow classifications are used. These classifications consumed heavy computational times and experienced individual assessments were required. The onset of CNNs (Convolution Neural Networks) which use several layers could identify or point out required objects photographs easily [18]. These approaches apply filters and convolute data in their processing layers i.e. filters are convoluted in each layer, generating a feature map that is utilised as input to subsequent layers. Their basic architecture enables them to process photographs as in pixel forms and thus achieve efficient classifications. These approaches have replaced multiple image processing steps of prior image analysis methods. Hence, based on reviews this study proposes a CNN based classification of LDs from CXRs.

DLBLDIT: Recent applications of DLTs have been focused on medical images including identification of LDs. The availability of computationally powerful machines allowed breakthroughs in medical image analysis/processing and many methods like pixel based learning have emerged. Instead of calculating features from segmented regions, this technique uses image pixels from input images directly, thus eliminating the need for segmentations or feature extractions. The suggested DLBLDIT scheme is shown in Figure 4.

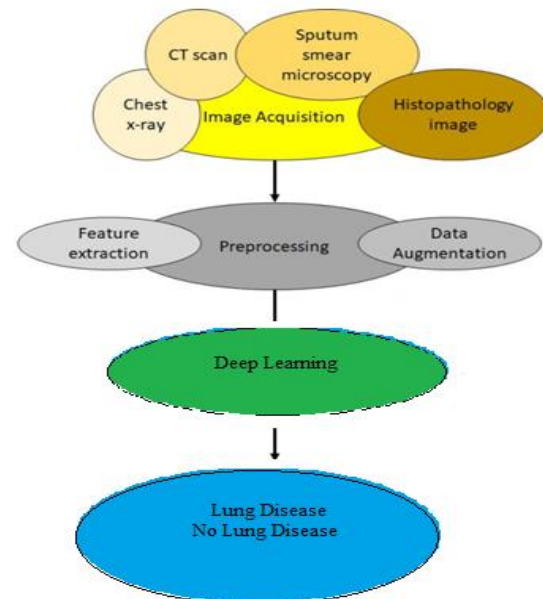


Fig. 4 – Scheme of proposed DLBLDIT

Pre-processing: DLBLDIT follows a set of sequential steps in pre-processing namely gray scale conversions, interpolations and normalization of images. Gray scale conversions can be done using average red, green and blue values by diving RGB values by three. Though theoretically, average method works, overflows errors occur in executions of the average method. Hence, this research work uses luminosity method for gray scale conversions. Figure 5 depicts the output of gray scale conversion using luminosity. Equation (1) depicts luminosity based gray scale conversion of images.

$$\text{Grayscale image} = ((0.3 * R) + (0.59 * G) + (0.11 * B)) \dots\dots\dots(1)$$



Fig. 5 - gray scale conversion using luminosity

Interpolation: Image resizing and interpolations are necessary for pixels increases/ decreases where Zooming operations increase pixel counts. Interpolations estimate unknown values using previously known values with their bi-directional operations. They attempt at estimating pixel intensities better based on the

pixel's adjacent pixel values. Interpolations can be categorized into adaptive or non-adaptive interpolations where Non-adaptive approaches consider all pixels as equals in their processing while adaptive approaches modify pixel's value based on interpolations. Examples of this kind of approaches include Nearest neighbours, bicubic, bilinear, sinc, spline and lanczos. Examples of adaptive interpolations include software like Qimage, PhotoZoom Pro, and Genuine Fractals. Most digital cameras come with optical and digital zooms where the former is achieved by zoom lens shifts resulting in greater magnifications of light while the latter decrease quality of photos by interpolations. Figure 6 depicts results of Interpolation where an image is blown ten times its size.

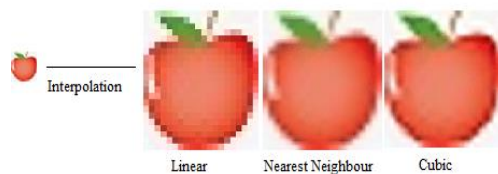


Fig. 6- Interpolation

Normalization of Images: DLT requires values in a certain format; therefore pixel values are scaled or normalized in the range $[0, 1]$. The procedures of standardizations scale pixel values for zero means with unit variations while scaling Pixel's centers zero means with unit variances are considered. This work standardizes input images by computing SDs (Standard Deviations) and means while training input image datasets.

Data augmentation: One main obstacle of binary classifications in training is imbalanced classes where one class instances in majority or greater numbers results in bias while DLTs show better performances when class instances are balanced. Hence, training datasets are enlarged artificially to reduce overfitting of samples and with same labels called augmentations. Image augmentations expand training datasets without requiring additional sample images and this is accomplished by altering original photos by certain procedures including rotations, translations, flips, zooms or inducing noises [19].

Classification: CNNs are DLTs that have been used effectively in image detecting patterns. They are made up of neurons similar to human brain's neurons with bias and weights. Each neuron receives multiple inputs while weights are computed from input weights. These weights are then used by activation functions for generating outputs. CNNs are very different other networks as they use convolution layers. Typical CNNs include Input, convolution, pooling and fully-connected layers. CNNs architecture is depicted in Figure 7 [20].

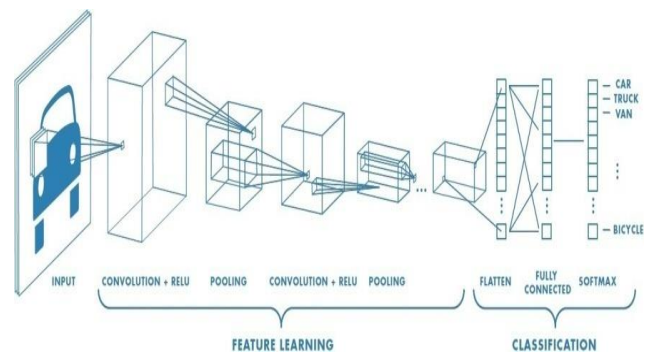


Fig. 7 - CNN Architecture

CNN's convolution layer use linear operations i.e. they multiply weights with inputs. These weights used in the operation are called kernels or filters where input data sizes are greater than that of kernels. The multiplied resultant is then summarized for singular outputs. Pooling layers gradually minimize data representations i.e. reduce computational parameters of the network and help in avoiding overfitting of data. ReLus (rectified linear units) of CNNs activate elements of previous layers using sigmoid functions. CNNs can achieve feature extractions as well as classifications where they extract features (also dimensionality reduction) from inputs using kernels/filters and thus generate feature maps which are used to identify important features. These features are then categorized as belonging to a class label based on their probabilities. CNNs have been specifically used in image categorizations/recognitions due to their ability to learn features automatically. Figure 8 depicts DLBDIT deep learning output.


```

Command Prompt - python blungs5.py
Epoch 3/18
7/7 [=====] - 32s 5s/step - loss: 0.5706 - accuracy: 0.8572 - val_loss: 5.0328 - val_accuracy: 0.5000
Epoch 00003: ReduceLROnPlateau reducing learning rate to 0.0003000000142492354.
Epoch 4/18
7/7 [=====] - 32s 5s/step - loss: 0.2920 - accuracy: 0.9131 - val_loss: 6.2192 - val_accuracy: 0.5000
Epoch 5/18
7/7 [=====] - 45s 6s/step - loss: 0.2151 - accuracy: 0.9141 - val_loss: 7.2572 - val_accuracy: 0.5000
Epoch 00005: ReduceLROnPlateau reducing learning rate to 9.000000427477062e-05.
Epoch 6/18
7/7 [=====] - 31s 5s/step - loss: 0.1999 - accuracy: 0.9529 - val_loss: 8.2690 - val_accuracy: 0.5000
Epoch 7/18
7/7 [=====] - 31s 4s/step - loss: 0.1779 - accuracy: 0.9047 - val_loss: 9.1784 - val_accuracy: 0.5000
Epoch 00007: ReduceLROnPlateau reducing learning rate to 2.700000040931627e-05.
Epoch 8/18
7/7 [=====] - 31s 4s/step - loss: 0.2599 - accuracy: 0.8883 - val_loss: 9.9548 - val_accuracy: 0.5000
Epoch 9/18
7/7 [=====] - 31s 4s/step - loss: 0.1850 - accuracy: 0.9269 - val_loss: 10.7289 - val_accuracy: 0.5000
Epoch 00009: ReduceLROnPlateau reducing learning rate to 8.10000013655517e-06.
Epoch 10/18
7/7 [=====] - 31s 4s/step - loss: 0.1234 - accuracy: 0.9401 - val_loss: 11.4232 - val_accuracy: 0.5000
Epoch 11/18
7/7 [=====] - 37s 5s/step - loss: 0.1801 - accuracy: 0.9224 - val_loss: 12.0045 - val_accuracy: 0.5000
Epoch 00011: ReduceLROnPlateau reducing learning rate to 2.429999949526973e-06.
Epoch 12/18
7/7 [=====] - 32s 4s/step - loss: 0.1688 - accuracy: 0.9271 - val_loss: 12.6279 - val_accuracy: 0.5000
Epoch 13/18
7/7 [=====] - 30s 4s/step - loss: 0.1538 - accuracy: 0.9413 - val_loss: 13.1067 - val_accuracy: 0.5000
Epoch 00013: ReduceLROnPlateau reducing learning rate to 1e-06.
Epoch 14/18
7/7 [=====] - 30s 4s/step - loss: 0.1861 - accuracy: 0.9488 - val_loss: 13.6375 - val_accuracy: 0.5000
Epoch 15/18
7/7 [=====] - 30s 4s/step - loss: 0.1568 - accuracy: 0.9416 - val_loss: 14.0582 - val_accuracy: 0.5000
Epoch 16/18
7/7 [=====] - 29s 4s/step - loss: 0.1565 - accuracy: 0.9543 - val_loss: 14.4860 - val_accuracy: 0.5000
Epoch 17/18
7/7 [=====] - 29s 4s/step - loss: 0.1953 - accuracy: 0.9024 - val_loss: 14.7888 - val_accuracy: 0.5000
Epoch 18/18
3/7 [=====] - ETA: 13s - loss: 0.2884 - accuracy: 0.8632

```

Fig. 8 - DLBLDIT Training Output

Results and Discussion:

Stagewise evaluation results of the suggested DLBLDIT approach executed on Python 3.9 using windows and with CXRs image Data Set downloaded from kaggle is displayed in this section. The dataset of 5863 images was organized into folders namely training, testing and validations and each with subfolders for each image category namely Diseased and Normal. Chest radiographs wof CXRs were checked for quality and CXRs which were unreadable/low quality were eliminated for the study. Clinical expert opinion was obtained on the selected images before being trained on CNNs.

DLBLDIT Pre-processing: The CXR images were pre-processed by converting them into gray scale using luminosity. Red color's wavelength is always greater amongst the three colors in an RGB image while green has the lowest wavelength. The contribution of red should be decreased and matched with the other colors. Hence, based on Equation (1) Red was set to 30, Green to 59 and blue to 11 in terms of distribution percentage. Even though images with digital zoom contain the same number of pixels, details are lesser than with optical zoom

and hence were interpolated for clarity. Gray scale conversions were followed by interpolations. This study used cubic interpolation as it produces a sharper interpolated image. Though Cubic interpolations are computationally more complex, and hence slower than linear interpolations, the quality of the resulting images was higher. The final step of pre-processing was normalization of image pixels. Images were rescaled in the range 0-1 from 0-255 to suit the proposed CNN training of images (Normalization). The rescale parameter was set to a ratio of 1/255 or 0.0039, which allows each pixel to be multiplied to attain the required range. Iterators with a batch size of 18 were then constructed for both the train and test datasets (Division of images in groups of 18). Each batch of the dataset has 18 photos with a height and width (rows and columns) of 28 pixels and a single channel, with new minimum and maximum pixel values of 0 and 1, respectively, thus confirming normalization was effective. Figure 9 depicts the gray scale outputs of CXRs.

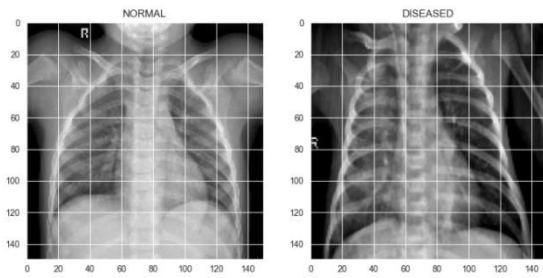


Fig. 9 – DLBLDIT Gray Scale Output

DLBLDIT Data Augmentation: Popular augmentation techniques include flips, random crops, translations, and rotations.. This research work applies data augmentations for making the proposed DLT model more robust. Data augmentations also overcome the hurdle of limited training samples by synthetically augmenting the training set. Flipping of images was used in this study as allow capture information about reflection invariances. Even weak algorithmic predictions can be accurate, when trained on small amount of samples [21]. Networks looking out for qualities that separate classes their predictions may go awry and can be avoided by flipping photos in opposite directions. This study used image

augmentations for effectively increasing overall performance of the suggested model. Figure 10 depicts Image data augmentations.

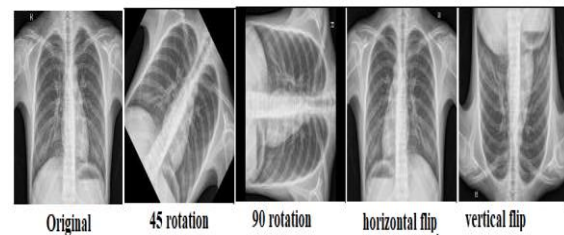


Fig. 10 – CXR Image augmentations

DLBLDIT Classification: The proposed DLBLDIT model was trained for 50 epochs using a dataset partitioned into 80% (training), 10% (validation), and 10% (testing). The image data was split into X (features) and y (labels). Using the batch size of 18 samples, resized (150 x 150 pixels), interpolated, normalized (Gray scale value from 0-255 to 0-1) and augmented (rotations) outputs were fed to CNNs for faster convergences. An Adam optimizer was used while categorical cross-entropy measured losses in pixel wise binary classifications. Figure 11 depicts the final output of DLBLDIT.

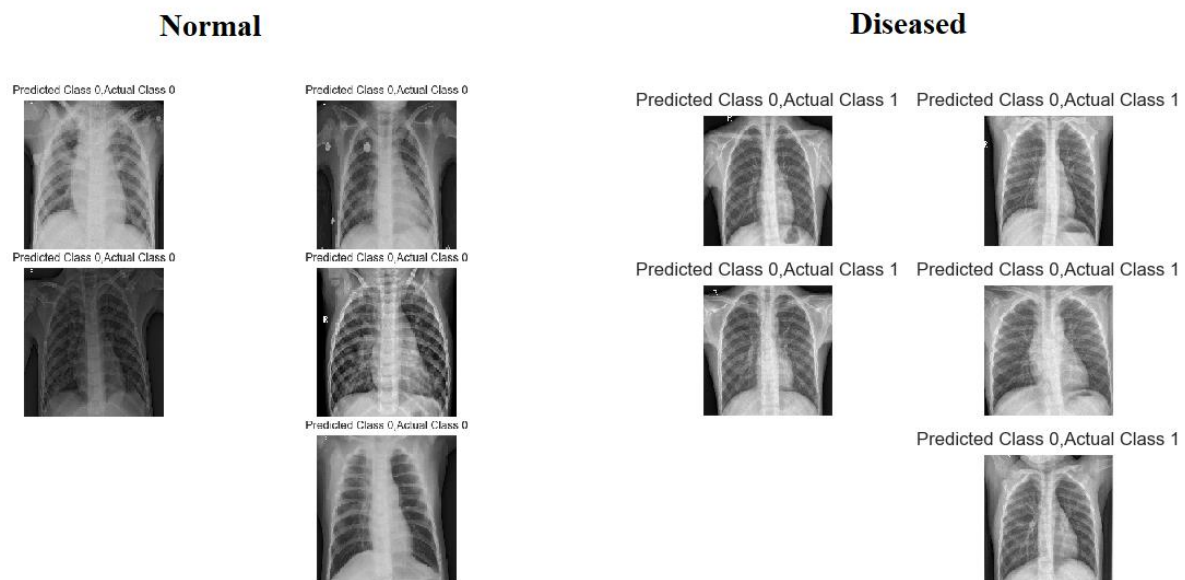


Fig. 11 – DLBLDIT Predictions from CXRs

DLBLDIT Performance: Learning (determining) suitable values for weights and bias of labelled samples is training. MLT models can learn in a supervised or

unsupervised manner, but learn to reduce loss (risk reductions) as wrong guesses result in losses. Errors also imply the inaccuracies of models where 0 implies forecasts are flawless

else it might be inaccurate. The basic aim of training is discovering ideal weights/bias with very marginal losses. Accuracies imply accurate classifications amongst all classifications while training accuracy refers to the accuracy achieved while training a model and test accuracy indicates a model's accuracy on unknown examples. Figure 12 depicts the results of DLBLDIT accuracy and losses in classifications.

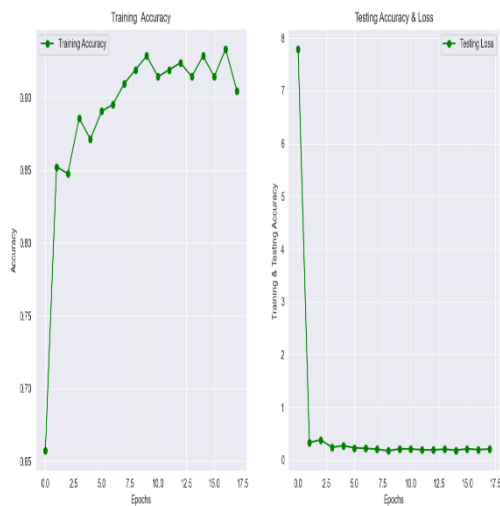


Fig. 12 - DLBLDIT classification values of training and testing

DLBLDIT Evaluation: For evaluating the model, the metrics of precision, recall, and F1 scores were used. These metrics are based on TPs (True Positives) which are correctly predicted positive class (prediction and actual both are positive) or CXRs predicted with LDs, TNs (True Negatives) which are correctly predicted negative class (prediction and actual both are negative) or CXRs that do not have LDs, FPs (False Positives) which gives wrong prediction of the negative class (predicted-positive, actual-negative) or CXRs wrongly predicted as LDs and FNs (False Negatives) which imply wrongly predicted positive class (predicted-negative, actual-positive) or CXRs not predicted as LDs but have LDs. Both precision and recall are crucial for information retrieval, where positive class matters the most. Precision is the measure where it indicates percentage that is truly positive out of all positive predictions. $\text{Precision} = \text{TP}/(\text{TP}+\text{FP})$.

Its value lies between 0 and 1. Recall is the measure for finding the percentage of positives predicted in total positives. $\text{Recall} = \text{TP}/(\text{TP}+\text{FN})$. F1 Score is the harmonic mean of precision and recall. It takes both false positive and false negatives into account. Therefore, it performs well on an imbalanced dataset. F1 score gives the same weightage to recall and precision. $\text{F1} = 2 * (\text{Precision} * \text{Recall}) / (\text{Precision} + \text{Recall})$. Table 1 lists the values of the performance metrics used for LDs detection from CXRs.

Table 1 – Performance Metrics of the Proposed DLBLDIT schema

	Precision	Recall	F1-Score	Count
CXRs with LDs	0.92	0.95	0.95	392
CXRs without LDs	0.94	0.85	0.88	236
Accuracy	0.93			628

It is evident from the above table that the proposed DLBLDIT has an overall accuracy of 93%. The scheme's precision values average .93, recall value is .90 and a F1 score of 91.5. This is mainly due to its steps in pre-processing and data augmentation prior to the application of CNNs for classification of LDs from CXR images.

Conclusion:

LDs has been affecting people increasingly including the latest pandemic COVID. In most cases LDs turn fatal increasing the mortality rates around the globe. Many researchers have proposed use of CAD based systems which use MLTs for early identification of LDs resulting in appropriate treatments and thus saving lives of LD patients. This study has proposed and demonstrated through implementations a LD classification pipeline based on deep learning and applied to CXRs. The proposed scheme DLBLDIT was evaluated based on the performance metrics of precision, recall and F1 scores. The proposed model shows reasonable precision of 92% and f-1 score of 0.93. This paper has focused on CXR image datasets for LDs classifications. Image driven approaches rely on pre-processing and segmentations while

the proposed approach achieved similar results in classification using data augmentations. This paper has thus suggested an implementable approach for detecting LDs from CXRs to assist pathologists in identifying LDs in their early stages. Additional pre-processing steps with segmentations and data augmentations could be tried to improve the precision and recall scores in future.

Reference

- [1] Bousquet, J. Global Surveillance, Prevention and Control of Chronic Respiratory Diseases; World Health Organization: Geneva, Switzerland, 2007; pp. 12–36.
- [2] Forum of International Respiratory Societies. The Global Impact of Respiratory Disease, 2nd ed.; European Respiratory Society, Sheffield, UK, 2017; pp. 5–42.
- [3] World Health Organization. Coronavirus Disease 2019 (COVID-19) Situation Report; Technical Report March; World Health Organization: Geneva, Switzerland, 2020.
- [4] Rahaman, M.M.; Li, C.; Yao, Y.; Kulwa, F.; Rahman, M.A.; Wang, Q.; Qi, S.; Kong, F.; Zhu, X.; Zhao, X. Identification of COVID-19 samples from chest X-Ray images using deep learning: A comparison of transfer learning approaches. *J. X-Ray Sci. Technol.* 2020, 28, 821–839.
- [5] American Thoracic Society. Diagnostic Standards and Classification of Tuberculosis in Adults and Children. *Am. J. Respir. Crit. Care Med.* 2000, 161, 1376–1395.
- [6] Setio, A.A.A.; Traverso, A.; de Bel, T.; Berens, M.S.; van den Bogaard, C.; Cerello, P.; Chen, H.; Dou, Q.; Fantacci, M.E.; Geurts, B.; et al. Validation, comparison, and combination of algorithms for automatic detection of pulmonary nodules in computed tomography images: The LUNA16 challenge. *Med. Image Anal.* 2017, 42, 1–13.
- [7] Yahiaoui, A.; Er, O.; Yumusak, N. A new method of automatic recognition for tuberculosis disease diagnosis using support vector machines. *Biomed. Res.* 2017, 28, 4208–4212.
- [8] Shen, D.; Wu, G.; Suk, H.I. Deep Learning in Medical Image Analysis. *Annu. Rev. Biomed. Eng.* 2017, 19, 221–248.
- [9] Wu, C.; Luo, C.; Xiong, N.; Zhang, W.; Kim, T.H. A Greedy Deep Learning Method for Medical Disease Analysis. *IEEE Access* 2018, 6, 20021–20030.
- [10] Ma, J.; Song, Y.; Tian, X.; Hua, Y.; Zhang, R.; Wu, J. Survey on deep learning for pulmonary medical imaging. *Front. Med.* 2019, 14, 450–469.
- [11] Webb, A. Introduction To Biomedical Imaging; John Wiley & Sons, Inc.: Hoboken, NJ, USA, 2003.
- [12] Kwan-Hoong, N.; Madan M, R. X ray imaging goes digital. *Br. Med J.* 2006, 333, 765–766.
- [13] Lopes, U.K.; Valiati, J.F. Pre-trained convolutional neural networks as feature extractors for tuberculosis detection. *Comput. Biol. Med.* 2017, 89, 135–143.
- [14] Ayan, E.; Ünver, H.M. Diagnosis of Pneumonia from Chest X-Ray Images using Deep Learning. *Sci. Meet. Electr.-Electron. Biomed. Eng. Comput. Sci.* 2019, 1–5.
- [15] Gordienko, Y.; Gang, P.; Hui, J.; Zeng, W.; Kochura, Y.; Alienin, O.; Rokovyi, O.; Stirenko, S. Deep Learning with Lung Segmentation and Bone Shadow Exclusion Techniques for Chest X-Ray Analysis of Lung Cancer. *Adv. Intell. Syst. Comput.* 2019, 638–647.
- [16] Salman, F.M.; Abu-naser, S.S.; Alajrami, E.; Abu-nasser, B.S.; Ashqar, B.A.M. COVID-19 Detection using Artificial Intelligence. *Int. J. Acad. Eng. Res.* 2020, 4, 18–25.
- [17] Gao, X.W.; James-reynolds, C.; Currie, E. Analysis of tuberculosis severity levels from CT pulmonary images based on enhanced residual deep learning architecture. *Neurocomputing* 2019, 392, 233–244.
- [18] Krizhevsky, A., Sutskever, I., and Hinton, G.E. (2017). ImageNet classification with deep convolutional neural networks. *Commun. ACM* 60, 84–90.
- [18] Gozes, O.; Frid, M.; Greenspan, H.; Patrick, D. Rapid AI Development Cycle for the Coronavirus (COVID-19) Pandemic: Initial Results for Automated

- Detection & Patient Monitoring using Deep Learning CT Image Analysis Article. arXiv 2020, arXiv:2003.05037
- [21] Domingos, P. A Few Useful Things to Know About Machine Learning. Commun. ACM 2012, 55, 78–87.
- [20] O’Shea, K.; Nash, R. An Introduction to Convolutional Neural Networks. arXiv 2015, arXiv:1511.08458v2.
- [21] Al-Ajlan, A.; Allali, A.E. CNN—MGP: Convolutional Neural Networks for Metagenomics Gene Prediction.